

000 001 002 003 004 005 NO ANSWER NEEDED: PREDICTING LLM ANSWER 006 ACCURACY FROM QUESTION-ONLY LINEAR PROBES 007 008 009

010 **Anonymous authors**
011

012 Paper under double-blind review
013
014
015
016
017
018
019
020
021
022
023
024
025
026

027 ABSTRACT 028

029 Do large language models (LLMs) anticipate when they will answer correctly?
030 To study this, we extract activations *after* a question is read but *before* any tokens
031 are generated, and train linear probes to predict whether the model’s forthcoming
032 answer will be correct. Across three open-source model families ranging from
033 7 to 70 billion parameters, projections on this “in-advance correctness direction”
034 trained on generic trivia questions predict success in distribution and on diverse
035 out-of-distribution knowledge datasets, indicating a deeper signal than dataset-
036 specific spurious features, and outperforming black-box baselines and verbalised
037 predicted confidence. Predictive power saturates in intermediate layers and, notably,
038 generalisation falters on questions requiring mathematical reasoning. Moreover,
039 for models responding “I don’t know”, doing so strongly correlates with the
040 probe score, indicating that the same direction also captures confidence. By
041 complementing previous results on truthfulness and other behaviours obtained
042 with probes and sparse auto-encoders, our work contributes essential findings to
043 elucidate LLM internals.
044
045

046 1 INTRODUCTION 047

048 Large language models (LLMs) internally encode information beyond what is immediately observable
049 in their output (Burns et al., 2022; Azaria & Mitchell, 2023; Marks & Tegmark, 2023; Burger
050 et al., 2024; Kudo et al., 2024; Goldowsky-Dill et al., 2025; Ferrando et al., 2025). Studies have
051 demonstrated that hidden activations can reveal latent concepts related to statement truthfulness
052 (Burns et al., 2022; Azaria & Mitchell, 2023; Marks & Tegmark, 2023; Burger et al., 2024), deception
053 (Goldowsky-Dill et al., 2025) and hallucination (Ferrando et al., 2025).
054

055 In this work, we investigate the structure of self-correctness representations in LLMs. Specifically,
056 we test the **Linear Representation Hypothesis** for correctness: does the residual stream activation
057 (captured immediately after processing a query) contain a direction that linearly separates questions
058 the model will answer correctly from those it will not? To do this, we employ a simple difference-of-
059 means linear probe in order to verify whether the correctness signal is accessible as a linear feature
060 of the representation space (Park et al., 2024), distinct from complex non-linear correlations (which
061 may be more complex than necessary to find such a signal in a production setup).
062

063 Empirically, our approach identifies the activation-space vector linking the average residual stream
064 activations for correctly answered questions to those for incorrectly answered ones (similar to Burger
065 et al., 2024’s method for statement truthfulness). We test our approach on open-source LLMs
066 spanning three families and ranging from 7 to 70 billion parameters, and we find:
067

- 068 • **Linear Separability:** We confirm that a correctness signal is indeed linearly separable in the
069 activation space. A simple linear probe trained on TriviaQA (Joshi et al., 2017) generalises
070 to domain-specific knowledge datasets, outperforming non-linear baselines (XGBoost) that
071 rely on model-independent question embeddings. This confirms that the internal activations
072 contain unique, linearly accessible information regarding the model’s own capabilities that
073 is not present in the general semantic embeddings of the input.
074
- 075 • **Factual vs. Arithmetic Misalignment:** While the direction generalizes across factual
076 domains (Trivia, Cities, People), it fails to generalize to mathematical reasoning (GSM8K).
077

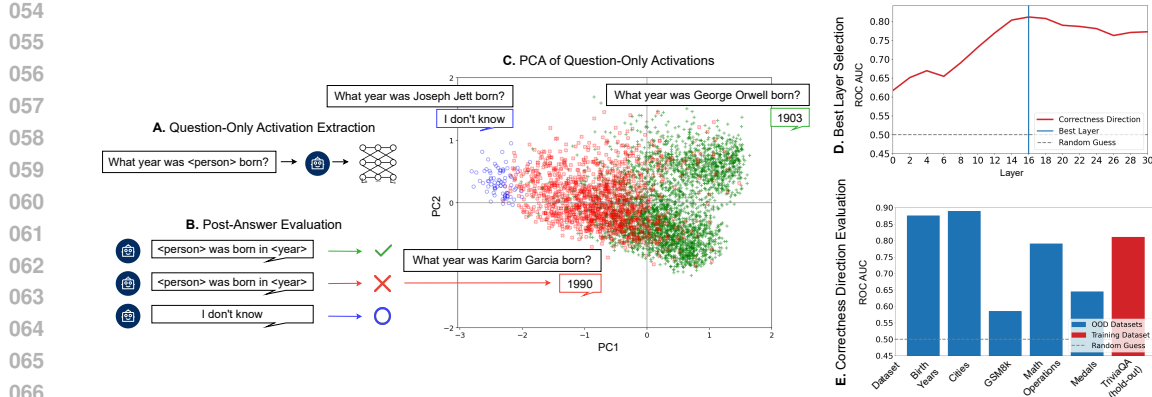


Figure 1: Proposed methodology to find the in-advance correctness direction. **(A)** Residual stream activations for all model layers are extracted at the last token of the question, prior to sampling. **(B)** Model answers are generated and evaluated against the ground truth. **(C)** The direction which mostly discriminates activations related to correct and incorrect answers is identified (the first two principal components at a specific layer are visualised). **(D)** The most discriminative layer is chosen. **(E)** The final correctness classifier is trained on the identified layer, and its out-of-distribution performance is assessed.

This indicates that "Factual Correctness" and "Arithmetic Correctness" may be distinct, orthogonal, or structurally misaligned vectors within the model.

- **Layer-wise Emergence:** For all models, the linear separability of correctness is low in early layers and saturates at intermediate transformer layers, suggesting the model's internal assessment of the prompt crystallizes mid-computation.
- **Correlation with Abstention:** For models that answer "I don't know" without being explicitly prompted, doing so correlates with the question's position along the in-advance correctness direction, suggesting this vector also captures an implicit confidence axis.
- **Scaling Trends:** The in-advance correctness signal is strongest and most consistent for the largest model we test (Llama 3.3 70B (Touvron et al., 2023)).

Overall, our analysis advances our understanding of how LLMs encode self-assessment, providing evidence for a general "Factual Correctness" direction while highlighting the structural distinctness of reasoning capabilities. Our codebase is accessible at <https://anonymous.4open.science/r/no-answer-needed>.

2 RELATED WORK

By avoiding generation from the model, our approach contrasts with self-confidence estimation methods (Shorinwa et al., 2024) that consider token-level output logits (Fadeeva et al., 2024), train additional modules to predict uncertainty (Kadavath et al., 2022), measure "semantic similarity" of multiple model generations (Kuhn et al., 2023), or ask models to verbalise their uncertainty (Lin et al., 2022; Kapoor et al., 2024). Notably, there is no consensus on the performance of these methods (Kapoor et al., 2024), which were shown to be brittle to shortcuts (Heindrich et al., 2025) and to yield inconsistent results across different methods (Pawitan & Holmes, 2024). Importantly, our probe is applicable to free-form answers, while not all the above approaches are. By avoiding model generation, our approach comes close to techniques training correctness predictors using model-independent features of the input ("assessors", Hernández-Orallo et al., 2022; Zhou et al., 2024; Pacchiardi et al., 2025), but differs from those in leveraging internal representations. On the other side, in contrast to our in-advance prediction of correctness, aforementioned works using model internals mostly focused on truthfulness of complete statements (Azaria & Mitchell, 2023; Burns et al., 2022; Marks & Tegmark, 2023; Burger et al., 2024; Bao et al., 2025) or other properties such as questions answerability (Heindrich et al., 2025), deception (Yang et al., 2024; Goldowsky-Dill

108 et al., 2025; Parrack et al., 2025), and when in a chain of thought internals predict the answer the
 109 model will eventually produce (Kudo et al., 2024).

110 The closest works to ours are Kadavath et al. (2022), which tested a similar probe to older proprietary
 111 models, but did not release any code to replicate or adapt their method, and Ferrando et al. (2025),
 112 which identified the latents of pre-trained Sparse Auto-Encoders (SAEs, Bricken et al., 2023) that
 113 best distinguish questions answered correctly from those answered incorrectly in small Gemma
 114 models (Team et al., 2024). As in these works, our work has the scientific goal of obtaining a better
 115 understanding of model internals, rather than optimizing for predictive power (which can be increased
 116 by combining internal embeddings with other features, as done in Kamath et al., 2020). Detailed
 117 discussion of the above and other related works can be found in Appendix A.

119 3 METHOD

120 3.1 PROBLEM FORMULATION

121 Let M be a LLM that, given an input prompt x , produces residual stream activations (after the final
 122 prompt token) $\{h^{(l)} \in \mathbb{R}^d\}$ at each layer $l = 1, \dots, L$. For that prompt, M can be used to produce
 123 (by autoregressive sampling) an output answer y . We define the correctness function $\text{Correct}(x, y)$ as
 124 a binary indicator of whether the answer is correct. Our objective is to learn a classifier f_w (where w
 125 indicates the classifier weights) that predicts the correctness label¹ from an intermediate activation
 126 $h^{(l)}(x)$, i.e.,

$$127 f_w(h^{(l)}(x)) \approx \mathbf{1}\{\text{Correct}(x, M(x))\}.$$

128 A key methodological decision in this work is the use of a simple linear classifier, specifically the
 129 difference-of-means direction, rather than more expressive non-linear probes (e.g., MLPs). We choose
 130 this to explicitly test if the correctness signal is *linearly separable*, rather than to maximize accuracy.
 131 If a simple linear direction w can successfully distinguish correct from incorrect inputs across diverse
 132 datasets, it suggests that "correctness" (or confidence) is represented as a coherent feature direction in
 133 the high-dimensional activation space, supporting the Linear Representation Hypothesis (Park et al.,
 134 2024). If complex non-linear classifiers were required, it would imply the information is encoded in a
 135 more entangled manner.

136 3.2 LEARNING A LATENT CORRECTNESS DIRECTION

137 Taking inspiration from Burger et al. (2024), we train a simple linear probe on fixed neural activations
 138 from a single layer obtained at the final prompt token. In particular, we partition the activations into
 139 two groups according to correctness. We summarize each class by the average activation vector over
 140 all examples in that class—one centroid for the incorrect outputs, μ_{false} , and one for the correct outputs,
 141 μ_{true} . Then, we define the correctness direction as the difference of the centroids: $w = \mu_{\text{true}} - \mu_{\text{false}}$.

142 For a given activation vector h , we then compute its correctness score by subtracting the mean of the
 143 centroids $\mu = \frac{1}{2}(\mu_{\text{false}} + \mu_{\text{true}})$ and projecting it on the normalized direction:

$$144 \text{score}(h) = \frac{(h - \mu)^\top w}{\|w\|}.$$

145 This score quantifies the alignment between the activation and the vector associated with correctness.
 146 Importantly, we do not apply a sigmoid to transform this score into a probability, nor use a
 147 threshold to assign class labels, although doing so is possible and straightforward. Instead, we assess
 148 the discriminative power of this direction by computing the Area Under the Receiver Operating
 149 Characteristic curve (AUROC), which is invariant under monotonic transformations of the scores and
 150 independent of any particular threshold since it measures performance across all possible cut-offs.

151 ¹If LLM answer generation is done with non-zero temperature, the correctness label inherently possesses
 152 non-zero aleatoric uncertainty (randomness). Thus, the classifier cannot perfectly predict the label, but it can
 153 approximate the random correctness label as accurately as possible, thereby reducing the epistemic uncertainty.
 154 In our experiments (Section 4), we set temperature to zero, so this consideration does not apply.

162 Therefore, our method does not produce a probabilistic classifier by default. It simply identifies a
 163 linear axis w in activation space that optimally separates correct from incorrect outputs, and uses the
 164 projections onto this axis to evaluate their separability.
 165

166 4 EXPERIMENTS AND RESULTS

167 4.1 SETUP

170 For each dataset–model pair, we collect a dataset of activations and correctness by prompting the
 171 model on every question x , extracting activations $h^{(l)}(x)$ (for layer l) at the question’s final token,
 172 sampling the answer y (temperature 0), and recording its correctness (0 or 1) against the gold answer.
 173 We then learn the direction as described in Section 3.2. To conduct the experiments, we used GPU
 174 resources on RunPod, employing approximately 60 hours of NVIDIA A100 time for evaluating the
 175 larger models, and around 100 hours of NVIDIA A40 time for the smaller models. We notice how
 176 most of the computational effort was spent in collecting the models’ activations: our probe’s training
 177 is a one-shot learning of a d -dimensional parameter vector on 10 k cached activations, and it takes
 178 less than three minutes on CPU; applying the probe involves a linear project, which is light-weight
 179 relatively to generation from a model.

180 4.1.1 DATASETS

182 We choose datasets where the performance of the considered models is in the mid range, so that
 183 enough samples are available for each of the two classes to accurately estimate the mean. Moreover,
 184 we avoid multiple-choice formats to prevent chance-correct answers from biasing our results. Instead,
 185 every dataset uses open-ended questions. Although some answer sets (e.g., countries or years) are
 186 bounded, they’re broad enough that the impact of random guessing is effectively negligible.

187 Therefore, we select two publicly available datasets and generate a few synthetic datasets (see Table 1).
 188 In particular, we derive our largest and most diverse dataset from a subset of TriviaQA (Joshi et al.,
 189 2017), which encompasses trivia-style questions covering a wide range of topics. To complement
 190 this, we construct three datasets from public tables to evaluate the in-advance correctness directions
 191 in specific factual-knowledge domains². The first³ asks which country a city belongs to; the second⁴
 192 requests to provide a notable person’s birth year; and the third⁵ queries which country won the gold
 193 medal in a specified sport at a particular edition of the Olympic Games. In addition, we construct
 194 our own dataset of arithmetic problems and employ GSM8K (Cobbe et al., 2021), a benchmark for
 195 mathematical reasoning.

196 4.1.2 LANGUAGE MODELS

198 We conduct our experiments on open state-of-the-art large language models (Table 2) varying in both
 199 training regimen and scale. We use three-shot prompting to mitigate answer formatting errors (exact
 200 prompts⁶ in Appendix B.8). The performance for each model on each dataset can be found in Table 5
 201 in Appendix B.1. Although we use a reasoning-trained model (Deepseek R1 Distill Qwen 32B), we
 202 do not employ reasoning-specific prompting and treat that identically to the other models.

204 4.1.3 BASELINES

205 To establish a point of reference to evaluate our approach, we consider two baseline approaches.

207 **Verbalized confidence.** We prompt each model to output a confidence score (0–100%) indicating its
 208 likelihood of answering each question correctly. The exact prompt can be found in Appendix B.8.

210 ²This is because we could not find existing datasets that simultaneously offered (i) free-form answers, (ii) a
 211 narrow topical scope that lets us measure cross-domain transfer, and (iii) fully automatic grading. Our Cities,
 212 Notable People and Medals datasets satisfy all three. Although small (6 k–16 k samples) they stress the probe
 213 with questions that differ markedly from TriviaQA’s trivia style.

214 ³Generated from the Geonames dataset from OpenDataSoft, licensed under CC BY 4.0.

215 ⁴Generated from the A Brief History of Human Time dataset from SciencesPo, licensed under CC-BY-SA.

⁵Generated from the Olympic History dataset on Kaggle, licensed under CC0 1.0.

⁶Exploratory investigation found the specific few-shot examples to not significantly affect performance.

216 Table 1: Details of the datasets employed in our work.
217

218 Dataset	219 N. samples	220 Source	221 Example
222 TriviaQA (Joshi et al., 2017)	223 60K	224 Public (subset)	225 What is the collective name of the four holy books of the Hindu religion?
226 Cities	227 10K	228 Custom (public data)	229 In which country is the city of Hungerford located?
230 Notable People	231 16K	232 Custom (public data)	233 What year was Thabo Mbeki (politician from South Africa) born?
234 Medals	235 9K	236 Custom (public data)	237 Which country won gold in Gymnastics Men’s Team All-Around in the 1948 Summer Olympics?
238 Math operations	239 6K	240 Custom	241 What is 5 plus 2?
242 GSM8K (Cobbe et al., 2021)	243 8K	244 Public	245 Natalia sold clips to 48 of her friends in April, and then she sold half as many clips in May. How many clips did Natalia sell altogether in April and May?

231 Table 2: Large Language Models used in our work, number of transformer layers and layer achieving
232 the best in-distribution AUC for the direction learned on TriviaQA (Section 4.2). The first layer is 0.
233

234 Model	235 N. layers	236 Best layer
237 Llama 3.1 8B	238 32	239 14
240 Llama 3.3 70B Instruct	241 80	242 76
243 Qwen 2.5 7B Instruct	244 28	245 22
246 DeepSeek R1 Distill Qwen 32B	247 64	248 44
249 Mistral 7B Instruct v0.3	250 32	251 16
252 Minstral 8B Instruct 2410	253 36	254 18

244 **Assessors.** We train LLM-specific binary classifiers using question text embeddings as model-
245 independent inputs and the corresponding evaluated model answers as labels. These black-box
246 *assessors* (Hernández-Orallo et al., 2022) predict an LLM’s performance on unseen questions
247 based on the question’s embedded features. Following Pacchiardi et al. (2024), we use OpenAI’s
248 `openai_text_embedding-3-large` model to obtain 3,072-dimensional question embeddings,
249 and we explore logistic regression and gradient boosted decision trees (Chen & Guestrin, 2016) to
250 establish linear and non-linear baseline assessors, respectively.

253

4.2 IDENTIFYING THE MOST DISCRIMINATIVE LAYER

255 For each LLM, we first identify the layer that most effectively discriminates between questions the
256 model answers correctly and those it answers incorrectly, with the approach in Section 3.2. We
257 perform this evaluation on TriviaQA because it offers a diverse array of questions across multiple
258 domains and complexity levels, which mitigates the risk of discovering an activation direction tied to
259 features merely correlated with model success rather than the model’s internal correctness prediction.
260 The remaining datasets are kept held-out for further evaluation. Appendix B.7 contains similar
261 experiments with all other datasets.

262 Thus, we dedicate a subset of 10,000 samples from TriviaQA exclusively to this step. We collect
263 activation samples every 2 layers for small (<10B parameters) models and every 4 for larger (>10B
264 parameters) models. On this data, for each model and layer, we perform 3-fold cross-validation and
265 train the model described in Section 3.2. Figure 2 presents the average AUROC over folds, and
266 Table 2 lists the resulting optimal layers. We observe that the early layers generally perform poorly
267 and performance saturates around the midpoint, with the optimal layer typically lying between the
268 midpoint and the final layer. This suggests the model’s understanding of its own answering ability
269 emerges progressively across layers, consistent with Ferrando et al. (2025) and Burger et al. (2024),
270 who also found representations in the middle layers to perform better for their task.

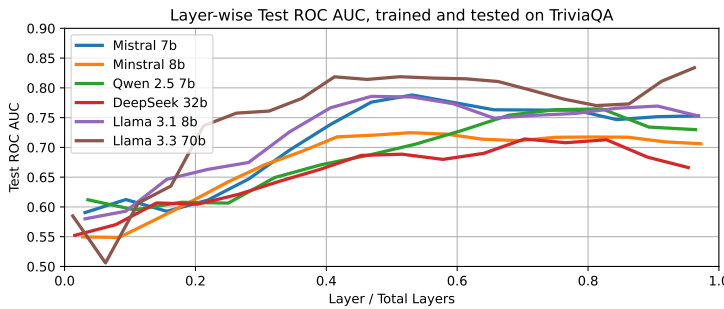
270
271
272
273
274
275
276
277
278
279
280

Figure 2: TriviaQA AUROC (average over 3 folds) across layers. We collect activations every 2 layers for small ($<10B$ parameters) models and every 4 layers for large ($>10B$ parameters) models.

4.3 CORRECTNESS DIRECTION GENERALIZATION

4.3.1 TRAINING ON TRIVIAQA

After identifying each model’s most informative layer on TriviaQA (Section 4.2), we evaluate whether the corresponding in-advance correctness direction generalises to other datasets. To do so, we split each dataset (excluding the first 10,000 elements of TriviaQA, used for layer selection, Section 4.2) into 5 folds, we train the correctness direction by iteratively considering 4 folds of TriviaQA and evaluating on the remaining one (for in-distribution performance) and on one individual fold for each of the out-of-distribution (OOD) datasets⁷. Similarly, we train the assessor baselines on TriviaQA and test them on the other datasets (the confidence baseline instead requires no training set). Table 3 reports the resulting average AUROC for each method: the correctness direction found on TriviaQA demonstrates significantly stronger generalization to all other datasets, with the exception of GSM8K, than the baseline methods (Section 4.1.3), despite being slightly outperformed by the logistic regression assessor in distribution. The direction approach improves on the best baseline by 10–22 AUROC points on Notable People, 5–18 points on Cities and 28–39 points on Math-Operations. On Medals, it remains the strongest method, but the margin contracts to 4–15 points, indicating that the gain diminishes on this harder multi-hop task. These patterns suggest that recognising one’s own competence scales with question difficulty and with model size: only the 70 B model shows a sizeable advantage on Medals. In contrast, no method can skilfully predict any of the models’ success on GSM8K well, confirming that the correctness signal does not transfer to arithmetic-reasoning tasks and indicating a potential limitation of current models. In Table 6, the standard deviation over the 5 folds for the learned direction is reported, showing that this is smaller than 0.035.

In Figure 5, we analyze the sample efficiency of the linear probe. Identifying the correctness direction requires very little data: robust performance is achieved with as few as 160 samples, and 2,560 samples are sufficient to match the performance obtained using the full 48,540 TriviaQA dataset. This high sample efficiency provides strong support for the Linear Representation Hypothesis: if the correctness signal were encoded in a complex, highly non-linear manifold, a simple difference-of-means probe would likely require significantly more data to generalize effectively. Notably, larger models require fewer samples to converge, suggesting that as model scale increases, the internal representation of correctness becomes more distinct and linearly accessible. Conversely, performance on GSM8K plateaus near random chance regardless of dataset size, reinforcing that the "Factual Correctness" direction is structurally misaligned with reasoning tasks, rather than simply being noisy or under-sampled.

We observe that while the Assessor baselines (trained on OpenAI embeddings) achieve slightly higher in-distribution scores, they suffer significant degradation out-of-distribution compared to our

⁷This is done so that the results are comparable to the ones obtained by training the correctness direction on the OOD dataset—which are too small for cross-validation to be applied—as discussed immediately below. Throughout training we always test on the held-out fold of the dataset whose AUROC we report, however, we train the probe in two alternative ways: (i) on the four remaining folds of TriviaQA (to assess cross-domain generalisation) or (ii) on the four folds of that same OOD dataset as an upper-bound. Hence, every cell of Table 3 compares methods on identical test questions, irrespective of training set.

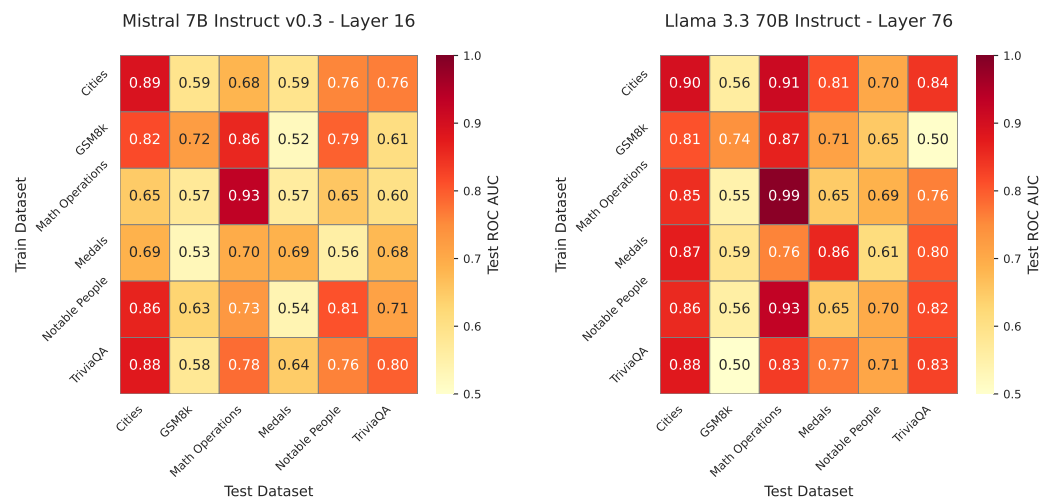


Figure 3: AUROC scores on each dataset for the direction learned on each dataset individually, for two selected models (others in Appendix B.5). Average AUROC over 5 folds is reported (Section 4.3).

linear probe. This contrast highlights the nature of the signal: the Assessor likely relies on spurious correlations in the semantic embeddings of the question text, which fail to hold across domain shifts. In contrast, our linear probe targets the model’s internal state. The fact that a simple linear direction on internal activations generalizes better than a non-linear XGBoost classifier on external embeddings (see Appendix B.3) confirms that the residual stream contains a genuine, transferable signal of self-competence that is not present in the surface semantics of the question alone.

4.3.2 TRAINING ON OTHER DATASETS

Next, to understand if the generalization is due to training on TriviaQA or if it can be instead obtained with any other dataset, we train and test the correctness direction on all dataset combinations, keeping the same folds as described above. We report results for Mistral 7B Instruct and Llama 3.3 70B in Figure 3 (other models in Appendix B.5). In some cases, the direction learned on the smaller specific datasets (such as Cities and Notable People) transfers well to others, but this does not always happen; at the same time, all datasets lead to decent in-distribution performance, with Medals being often the lowest one (even considering the other models in Appendix B.5). In Appendix B.6, we further report the cosine similarity between the directions learned on the different datasets, which shows how the directions learned on the small datasets are mostly orthogonal, except for a few cases (Cities and Notable People), which are also more aligned with the direction learned on TriviaQA. These observations suggest that, for certain datasets, the learned direction captures dataset-specific cues correlated with correctness rather than correctness itself⁸. Over all models, moreover, the direction learned from TriviaQA shows the strongest generalisation (except for GSM8K and Medals, as already discussed above), likely because its diverse nature makes it less likely to contain exploitable dataset-specific patterns. Further, comparing the models, we find that Llama 3.3 70B generalizes well across the largest number of train–test dataset pairs, suggesting that this larger model has a more consistent correctness direction.

4.4 QUALITATIVE INVESTIGATION

Alongside our main experiments, we observe several behaviours and patterns that are not easily quantifiable but nonetheless offer a valuable insight into the quality of the direction we find. In particular, Section 4.5 shows how some models, despite being urged to give an answer in a specific format, produced some form of abstention; these answers are located on the negative extreme of the

⁸For context, QA accuracies on GSM8K range from 10.7% to 44.3% and on Cities from 45.8% to 80.3% (Table 5), so all datasets have substantial mass in both classes, an ‘always correct’ baseline would have AUROC 0.5 by construction.

378
 379 Table 3: AUROC for each dataset, model and method. All directions are trained on the TriviaQA
 380 dataset on the optimal layer found in Section 4.2. Average AUROC over 5 folds is reported (Sec-
 381 tion 4.3, variance reported in Table 6). For the assessors, we only report the best performing one
 382 (logistic regression; all results in Appendix B.3). As the probes are trained on finite samples, weak or
 383 noisy signal might result in AUROC slightly below 0.5.

384 385 Model	386 Method	387 Test dataset					
		388 TriviaQA	389 N. people	390 Cities	391 Math ops.	392 Medals	393 GSM8K
394 Llama 3.1 8B	395 Assessor	0.852	0.630	0.663	0.528	0.623	0.558
	396 Verb. conf.	0.502	0.499	0.500	0.623	0.500	0.540
	397 Direction	0.804	0.722	0.732	0.858	0.680	0.534
398 Llama 3.3 70B	399 Assessor	0.759	0.583	0.672	0.449	0.568	0.573
	400 Verb. conf.	0.580	0.594	0.694	0.913	0.665	0.598
	401 Instruct	0.826	0.708	0.880	0.835	0.770	0.499
402 Qwen 2.5 7B	403 Assessor	0.807	0.723	0.708	0.400	0.622	0.584
	404 Verb. conf.	0.643	0.637	0.758	0.517	0.531	0.513
	405 Direction	0.758	0.800	0.842	0.837	0.586	0.601
406 DeepSeek R1	407 Assessor	0.790	0.709	0.663	0.337	0.601	0.576
	408 Distill Qwen 32B	409 Verb. conf.	0.619	0.605	0.577	0.499	0.563
	410 Direction	0.735	0.825	0.879	0.847	0.638	0.552
411 Mistral 7B	412 Assessor	0.846	0.673	0.710	0.493	0.638	0.559
	413 Instruct v0.3	414 Verb. conf.	0.570	0.625	0.705	0.617	0.558
	415 Direction	0.796	0.760	0.880	0.782	0.645	0.579
416 Minstral 8B	417 Assessor	0.789	0.623	0.682	0.454	0.626	0.598
	418 Instruct 2410	419 Verb. conf.	0.515	0.500	0.554	0.500	0.502
	420 Direction	0.734	0.680	0.840	0.844	0.670	0.578

406
 407 correctness direction, and suggests that our correctness-prediction direction also captures abstention.
 408 Instead, Section 4.6 contains a manual investigation of correct and incorrect answers with the highest
 409 positive and negative values of correctness scores, showing patterns which intuitively align with
 410 confidence scores (e.g., wrong answers with high scores being near-misses where the model fails by
 411 one or a few years).

412 4.5 LOCATION OF “I DON’T KNOW” RESPONSES

413
 414 Some of the models we tested, despite being urged to give a specific answer format by our prompt,
 415 produced answers of the form “I don’t know” (IDK) or similar to some questions. When training
 416 the correctness direction, these were considered as incorrect answers. By visualizing (Figure 4)
 417 the distribution of activation projections on the correctness direction at the optimal layer found in
 418 Section 4.2, we see that the questions where the model answers IDK are consistently located more
 419 at the negative extreme of the correctness direction than the questions where the model attempts an
 420 answer but fails. This behaviour demonstrates that the overall internal state, causally upstream of the
 421 model outputting “I don’t know” or attempt an answer, is strongly captured in the direction that we
 422 find. This aligns with Ferrando et al. (2025)’s finding of “knowledge-awareness” directions causally
 423 affecting answer refusal. Thus, our “correctness-prediction” direction could also be interpreted as a
 424 confidence direction: the model will only say that it doesn’t know if its confidence on whether it can
 425 answer the question is very low.

426 4.6 MANUAL INVESTIGATION OF EXTREME VALUES

427
 428 Finally, we report in Table 4 the correct and incorrect answer with the highest positive and negative
 429 values of correctness scores for Mistral 7B Instruct. The patterns we observe are intuitive: among
 430 the incorrect answers with low confidence scores, we find IDK responses, which is consistent with
 431 the behaviour discussed in Section 4.5. For wrong answers with high scores, we often see questions
 for which the model fails by one or a few years, and the correct answers with the highest confidence

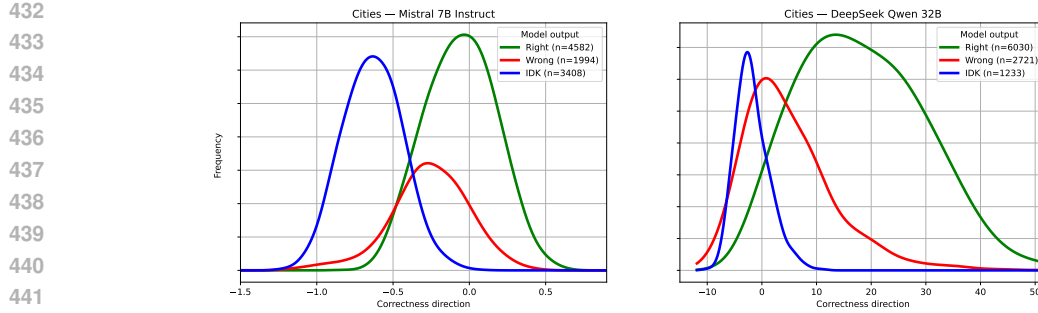


Figure 4: Distribution of values of activation projections on the correctness direction from TriviaQA, grouped by produced answer (right, wrong, “I don’t know”), for a selection of models and datasets.

involve very well-known individuals, which aligns with the interpretation that we are finding a confidence direction.

Table 4: Questions of the Notable People dataset with the most extreme values on the correctness direction trained on TriviaQA for Mistral 7B Instruct.

		Person	Answer (Correct)
Wrong answers	Low scores	Victoria (Royal Family from Germany) Yokozuna (wrestler from US)	IDK (1840) 1972 (1966)
	High scores	Kazimir Malevich (painter from Russia) A. A. Milne (writer from United Kingdom)	1961 (1962) 1892 (1882)
Right answers	Low scores	Jim Carter (actor from United Kingdom) David Keith (film-maker from US)	1948 (1948) 1954 (1954)
	High scores	Charles Darwin (biologist from United Kingdom) Albert Einstein (physicist from Germany)	1809 (1809) 1879 (1879)

5 CONCLUSION

We have provided evidence for the Linear Representation Hypothesis regarding LLM self-correctness. By analyzing the residual stream before token generation, we identified a “correctness direction” that is linearly separable and generalizes across diverse factual tasks. Our comparison with external-embedding baselines confirms that this signal is intrinsic to the model’s internal state. However, the failure to generalize to mathematical reasoning suggests that factual retrieval and arithmetic reasoning may rely on distinct internal verification mechanisms. These findings advance our scientific understanding of how LLMs encode their own capabilities and limitations.

Specifically: (1) we provide evidence that LLMs embed a latent correctness signal mid-computation; (2) we show that a simple linear probe can extract this signal (providing evidence for linear separability), yielding generalisation across knowledge datasets; (3) we highlight the limits of this approach, suggesting that deeper reasoning and arithmetic capabilities are not as easily captured in activations; (4) we find a stronger signal for the largest model we test (Llama 3.3 70B), suggesting that larger models may better predict their correctness, and (5) we demonstrate this direction aligns with abstention behaviour in models that say “I don’t know,” supporting its interpretation as a latent confidence axis.

This work contributes to mechanistic interpretability by identifying a meaningful confidence direction within LLM activations, corroborating recent works with sparse auto-encoders (Ferrando et al., 2025). It also complements studies of truthfulness and hallucination, suggesting that models encode internal notions of confidence—even before answer generation—and truthfulness that are both general and accessible.

486 Our findings have relevance for both AI safety and practical deployment. As LLMs are increasingly
 487 used in high-stakes settings, low-cost internal signals of impending failure offer a path toward
 488 safer, more robust systems. The correctness direction, combined with an ensemble of other black-
 489 and white-box methods, could inform early stopping, fallback mechanisms, or human-in-the-loop
 490 protocols, particularly where generating unreliable outputs is costly or dangerous.
 491

492 6 LIMITATIONS

493
 494 **Correctness is represented as a binary label from a single sample.** This ignores stochasticity of
 495 answer generation and the existence of questions with ambiguous or nuanced answers that cannot
 496 be captured by a single true/false label. Future work might involve generating multiple samples or
 497 assigning real-valued correctness scores to obtain a more robust estimate of expected correctness; a
 498 natural extension for reasoning specifically is to probe along the reasoning trajectory and to compare
 499 linear probes against stronger baselines on reasoning-heavy datasets.

500 **Linear probes may underestimate predictive power.** We used linear representations as a model can
 501 more conceivably access them during answer generation, but higher-capacity non-linear classifiers
 502 may yield greater predictive power. Further, the probes are targeted towards a pre-generation factual
 503 correctness signal, which is not a memorisation-free notion of correctness, and should be carefully
 504 evaluated in future work.

505 **Model diversity and scale.** We evaluate on six open-source models from three families, up to 70B
 506 parameters. While this spans a wide range, results may not fully generalize to proprietary models,
 507 alternative architectures (e.g., mixture-of-experts), or future frontier systems. Only a single large
 508 model (70B) was used due to compute limitations.

509 **Layer selection is performed on a single dataset.** We identify the most discriminative layer for
 510 each model using a single large general dataset (TriviaQA). To ensure the generality of our findings,
 511 we could repeat the layer choice on other large generalist datasets.

513 7 REPRODUCIBILITY STATEMENT

515
 516 We provide the codebase, raw datasets, and generated datasets to fully reproduce our work at <https://anonymous.4open.science/r/no-answer-needed>. The recorded activations for all
 517 our models will be made available upon that paper's acceptance (as their size prevents us from adding
 518 them to the anonymous repository).

521 REFERENCES

522 Amos Azaria and Tom Mitchell. The internal state of an LLM knows when it's lying. In
 523 Houda Bouamor, Juan Pino, and Kalika Bali (eds.), *Findings of the Association for Compu-
 524 tational Linguistics: EMNLP 2023*, pp. 967–976, Singapore, December 2023. Association
 525 for Computational Linguistics. doi: 10.18653/v1/2023.findings-emnlp.68. URL <https://aclanthology.org/2023.findings-emnlp.68/>.

527 Yuntai Bao, Xuhong Zhang, Tianyu Du, Xinkui Zhao, Zhengwen Feng, Hao Peng, and Jianwei Yin.
 528 Probing the geometry of truth: Consistency and generalization of truth directions in llms across
 529 logical transformations and question answering tasks. *arXiv preprint arXiv:2506.00823*, 2025.

530 Daniel Beaglehole, Adityanarayanan Radhakrishnan, Enric Boix-Adserà, and Mikhail Belkin. Ag-
 531 gregate and conquer: detecting and steering llm concepts by combining nonlinear predictors over
 532 multiple layers. *arXiv preprint arXiv:2502.03708*, 2025.

533 Trenton Bricken, Adly Templeton, Joshua Batson, Brian Chen, Adam Jermyn, Tom Conerly, Nick
 534 Turner, Cem Anil, Carson Denison, Amanda Askell, Robert Lasenby, Yifan Wu, Shauna Kravec,
 535 Nicholas Schiefer, Tim Maxwell, Nicholas Joseph, Zac Hatfield-Dodds, Alex Tamkin, Karina
 536 Nguyen, Brayden McLean, Josiah E Burke, Tristan Hume, Shan Carter, Tom Henighan, and
 537 Christopher Olah. Towards monosemanticity: Decomposing language models with dictionary
 538 learning. *Transformer Circuits Thread*, 2023. <https://transformer-circuits.pub/2023/monosemantic-features/index.html>.

540 Lennart Burger, Fred A Hamprecht, and Boaz Nadler. Truth is universal: Robust detection of lies in
 541 llms. *Advances in Neural Information Processing Systems*, 37:138393–138431, 2024.
 542

543 Collin Burns, Haotian Ye, Dan Klein, and Jacob Steinhardt. Discovering latent knowledge in language
 544 models without supervision. *arXiv preprint arXiv:2212.03827*, 2022.
 545

546 Arslan Chaudhry, Sridhar Thiagarajan, and Dilan Gorur. Finetuning language models to emit
 547 linguistic expressions of uncertainty. *arXiv preprint arXiv:2409.12180*, 2024.
 548

549 Tianqi Chen and Carlos Guestrin. Xgboost: A scalable tree boosting system. In *Proceedings of the*
 550 *22nd ACM SIGKDD international conference on knowledge discovery and data mining*, pp. 785–794,
 551 2016.
 552

553 Karl Cobbe, Vineet Kosaraju, Mo Bavarian, Mark Chen, Heewoo Jun, Lukasz Kaiser, Matthias
 554 Plappert, Jerry Tworek, Jacob Hilton, Reiichiro Nakano, Christopher Hesse, and John Schulman.
 555 Training verifiers to solve math word problems. *ArXiv*, abs/2110.14168, 2021. URL <https://api.semanticscholar.org/CorpusID:239998651>.
 556

557 Ekaterina Fadeeva, Aleksandr Rubashevskii, Artem Shelmanov, Sergey Petrakov, Haonan Li, Hamdy
 558 Mubarak, Evgenii Tsymbalov, Gleb Kuzmin, Alexander Panchenko, Timothy Baldwin, Preslav
 559 Nakov, and Maxim Panov. Fact-checking the output of large language models via token-level
 560 uncertainty quantification. In Lun-Wei Ku, Andre Martins, and Vivek Srikumar (eds.), *Findings of*
 561 *the Association for Computational Linguistics: ACL 2024*, pp. 9367–9385, Bangkok, Thailand,
 562 August 2024. Association for Computational Linguistics. doi: 10.18653/v1/2024.findings-acl.558.
 563 URL <https://aclanthology.org/2024.findings-acl.558/>.
 564

565 Javier Ferrando, Oscar Balcells Obeso, Senthooran Rajamanoharan, and Neel Nanda. Do i know
 566 this entity? knowledge awareness and hallucinations in language models. In *The Thirteenth*
 567 *International Conference on Learning Representations*, 2025. URL <https://openreview.net/forum?id=WCRQFlji2q>.
 568

569 Yarin Gal and Zoubin Ghahramani. Dropout as a Bayesian approximation: Representing model
 570 uncertainty in deep learning. In *international conference on machine learning*, pp. 1050–1059.
 571 PMLR, 2016.
 572

573 Nicholas Goldowsky-Dill, Bilal Chughtai, Stefan Heimersheim, and Marius Hobbahn. Detecting
 574 strategic deception using linear probes. *arXiv preprint arXiv:2502.03407*, 2025.
 575

576 Daniela Gottesman and Mor Geva. Estimating knowledge in large language models without generating
 577 a single token. *arXiv preprint arXiv:2406.12673*, 2024.
 578

579 Chuan Guo, Geoff Pleiss, Yu Sun, and Kilian Q Weinberger. On calibration of modern neural
 580 networks. In *International conference on machine learning*, pp. 1321–1330. PMLR, 2017.
 581

582 Lovis Heindrich, Philip Torr, Fazl Barez, and Veronika Thost. Do sparse autoencoders generalize? A
 583 case study of answerability. *arXiv preprint arXiv:2502.19964*, 2025.
 584

585 José Hernández-Orallo, Wout Schellart, and Fernando Martínez-Plumed. Training on the test set:
 586 Mapping the system-problem space in AI. In *Proceedings of the AAAI conference on artificial*
 587 *intelligence*, volume 36, pp. 12256–12261, 2022.
 588

589 Ziwei Ji, Delong Chen, Etsuko Ishii, Samuel Cahyawijaya, Yejin Bang, Bryan Wilie, and Pascale Fung.
 590 Llm internal states reveal hallucination risk faced with a query. *arXiv preprint arXiv:2407.03282*,
 591 2024.
 592

593 Mandar Joshi, Eunsol Choi, Daniel Weld, and Luke Zettlemoyer. TriviaQA: A large scale
 594 distantly supervised challenge dataset for reading comprehension. In Regina Barzilay and
 595 Min-Yen Kan (eds.), *Proceedings of the 55th Annual Meeting of the Association for Com-
 596 putational Linguistics (Volume 1: Long Papers)*, pp. 1601–1611, Vancouver, Canada, July
 597 2017. Association for Computational Linguistics. doi: 10.18653/v1/P17-1147. URL <https://aclanthology.org/P17-1147/>.
 598

594 Laurent Valentin Jospin, Hamid Laga, Farid Boussaid, Wray Buntine, and Mohammed Bennamoun.
 595 Hands-on bayesian neural networks—a tutorial for deep learning users. *IEEE Computational*
 596 *Intelligence Magazine*, 17(2):29–48, 2022.

597 Saurav Kadavath, Tom Conerly, Amanda Askell, Tom Henighan, Dawn Drain, Ethan Perez, Nicholas
 598 Schiefer, Zac Hatfield-Dodds, Nova DasSarma, Eli Tran-Johnson, Scott Johnston, Sheer El Showk,
 599 Andy Jones, Nelson Elhage, Tristan Hume, Anna Chen, Yuntao Bai, Sam Bowman, Stanislav Fort,
 600 Deep Ganguli, Danny Hernandez, Josh Jacobson, Jackson Kernion, Shauna Kravec, Liane Lovitt,
 601 Kamal Ndousse, Catherine Olsson, Sam Ringer, Dario Amodei, Tom Brown, Jack Clark, Nicholas
 602 Joseph, Ben Mann, Sam McCandlish, Chris Olah, and Jared Kaplan. Language models (mostly)
 603 know what they know. *CoRR*, abs/2207.05221, 2022. URL <https://doi.org/10.48550/arXiv.2207.05221>.

604 Amita Kamath, Robin Jia, and Percy Liang. Selective question answering under domain shift. In
 605 Dan Jurafsky, Joyce Chai, Natalie Schluter, and Joel Tetreault (eds.), *Proceedings of the 58th*
 606 *Annual Meeting of the Association for Computational Linguistics*, pp. 5684–5696, Online, July
 607 2020. Association for Computational Linguistics. doi: 10.18653/v1/2020.acl-main.503. URL
 608 <https://aclanthology.org/2020.acl-main.503/>.

609 Sanyam Kapoor, Nate Gruver, Manley Roberts, Katherine M. Collins, Arka Pal, Umang Bhatt,
 610 Adrian Weller, Samuel Dooley, Micah Goldblum, and Andrew Gordon Wilson. Large language
 611 models must be taught to know what they don’t know. In *The Thirty-eighth Annual Conference on*
 612 *Neural Information Processing Systems*, 2024. URL <https://openreview.net/forum?id=QzvWyggrYB>.

613 Been Kim, Martin Wattenberg, Justin Gilmer, Carrie Cai, James Wexler, Fernanda Viegas, et al.
 614 Interpretability beyond feature attribution: Quantitative testing with concept activation vectors
 615 (tcav). In *International conference on machine learning*, pp. 2668–2677. PMLR, 2018.

616 Keito Kudo, Yoichi Aoki, Tatsuki Kuribayashi, Shusaku Sone, Masaya Taniguchi, Ana Bras-
 617 sard, Keisuke Sakaguchi, and Kentaro Inui. Think-to-talk or talk-to-think? when llms come
 618 up with an answer in multi-step reasoning. *ArXiv*, abs/2412.01113, 2024. URL <https://api.semanticscholar.org/CorpusID:274436653>.

619 Lorenz Kuhn, Yarin Gal, and Sebastian Farquhar. Semantic uncertainty: Linguistic invariances for
 620 uncertainty estimation in natural language generation. *arXiv preprint arXiv:2302.09664*, 2023.

621 Bruce W. Lee, Inkit Padhi, Karthikeyan Natesan Ramamurthy, Erik Miehling, Pierre Dognin, Manish
 622 Nagireddy, and Amit Dhurandhar. Programming refusal with conditional activation steering.
 623 In *The Thirteenth International Conference on Learning Representations*, 2025. URL <https://openreview.net/forum?id=Oi47wc10sm>.

624 Stephanie Lin, Jacob Hilton, and Owain Evans. Teaching models to express their uncertainty in
 625 words. *Transactions on Machine Learning Research*, 2022. ISSN 2835-8856. URL <https://openreview.net/forum?id=8s8K2UZGTZ>.

626 Samuel Marks and Max Tegmark. The geometry of truth: Emergent linear structure in large
 627 language model representations of true/false datasets. *ArXiv*, abs/2310.06824, 2023. URL
 628 <https://api.semanticscholar.org/CorpusID:263831277>.

629 Jord Nguyen, Khiem Hoang, Carlo Leonardo Attubato, and Felix Hofstätter. Probing evaluation
 630 awareness of language models. *arXiv preprint arXiv:2507.01786*, 2025.

631 Lorenzo Pacchiardi, Lucy G. Cheke, and José Hernández-Orallo. 100 instances is all you need:
 632 predicting the success of a new LLM on unseen data by testing on a few instances, 2024. URL
 633 <https://arxiv.org/abs/2409.03563>.

634 Lorenzo Pacchiardi, Konstantinos Voudouris, Ben Slater, Fernando Martínez-Plumed, José
 635 Hernández-Orallo, Lexin Zhou, and Wout Schellaert. PredictaBoard: Benchmarking LLM score
 636 predictability, 2025. URL <https://arxiv.org/abs/2502.14445>.

637 Kiho Park, Yo Joong Choe, and Victor Veitch. The linear representation hypothesis and the geometry
 638 of large language models, 2024. URL <https://arxiv.org/abs/2311.03658>.

648 Avi Parrack, Carlo Leonardo Attubato, and Stefan Heimersheim. Benchmarking deception probes
 649 via black-to-white performance boosts. *arXiv preprint arXiv:2507.12691*, 2025.
 650

651 Yudi Pawitan and Chris Holmes. Confidence in the reasoning of large language models. *arXiv
 652 preprint arXiv:2412.15296*, 2024.

653 Dylan Sam, Marc Finzi, and J. Zico Kolter. Predicting the performance of black-box llms through
 654 self-queries, 2025. URL <https://arxiv.org/abs/2501.01558>.
 655

656 Wout Schellaert, Fernando Martínez-Plumed, and José Hernández-Orallo. Analysing the predictability
 657 of language model performance. *ACM Transactions on Intelligent Systems and Technology*, 2024.
 658

659 Ola Shorinwa, Zhiting Mei, Justin Lidard, Allen Z Ren, and Anirudha Majumdar. A survey on
 660 uncertainty quantification of large language models: Taxonomy, open research challenges, and
 661 future directions. *arXiv preprint arXiv:2412.05563*, 2024.

662 Vaishnavi Shrivastava, Ananya Kumar, and Percy Liang. Language models prefer what they know:
 663 Relative confidence estimation via confidence preferences. *arXiv preprint arXiv:2502.01126*, 2025.
 664

665 Aviv Slobodkin, Omer Goldman, Avi Caciularu, Ido Dagan, and Shauli Ravfogel. The curious case
 666 of hallucinatory (un) answerability: Finding truths in the hidden states of over-confident large
 667 language models. *arXiv preprint arXiv:2310.11877*, 2023.

668 Ben Snyder, Marius Moisescu, and Muhammad Bilal Zafar. On early detection of hallucinations in
 669 factual question answering. In *Proceedings of the 30th ACM SIGKDD Conference on Knowledge
 Discovery and Data Mining*, pp. 2721–2732, 2024.

670 Gemma Team, Morgane Riviere, Shreya Pathak, Pier Giuseppe Sessa, Cassidy Hardin, Surya
 671 Bhupatiraju, Léonard Hussenot, Thomas Mesnard, Bobak Shahriari, Alexandre Ramé, Johan
 672 Ferret, Peter Liu, Pouya Tafti, Abe Friesen, Michelle Casbon, Sabela Ramos, Ravin Kumar,
 673 Charline Le Lan, Sammy Jerome, Anton Tsitsulin, Nino Vieillard, Piotr Stanczyk, Sertan Girgin,
 674 Nikola Momchev, Matt Hoffman, Shantanu Thakoor, Jean-Bastien Grill, Behnam Neyshabur,
 675 Olivier Bachem, Alanna Walton, Aliaksei Severyn, Alicia Parrish, Aliya Ahmad, Allen Hutchison,
 676 Alvin Abdagic, Amanda Carl, Amy Shen, Andy Brock, Andy Coenen, Anthony Laforge, Antonia
 677 Paterson, Ben Bastian, Bilal Piot, Bo Wu, Brandon Royal, Charlie Chen, Chintu Kumar, Chris
 678 Perry, Chris Welty, Christopher A. Choquette-Choo, Danila Sinopalnikov, David Weinberger,
 679 Dimple Vijaykumar, Dominika Rogozińska, Dustin Herbison, Elisa Bandy, Emma Wang, Eric
 680 Noland, Erica Moreira, Evan Senter, Evgenii Eltyshev, Francesco Visin, Gabriel Rasskin, Gary
 681 Wei, Glenn Cameron, Gus Martins, Hadi Hashemi, Hanna Klimczak-Plucińska, Harleen Batra,
 682 Harsh Dhand, Ivan Nardini, Jacinda Mein, Jack Zhou, James Svensson, Jeff Stanway, Jetha
 683 Chan, Jin Peng Zhou, Joana Carrasqueira, Joana Iljazi, Jocelyn Becker, Joe Fernandez, Joost
 684 van Amersfoort, Josh Gordon, Josh Lipschultz, Josh Newlan, Ju yeong Ji, Kareem Mohamed,
 685 Kartikeya Badola, Kat Black, Katie Millican, Keelin McDonell, Kelvin Nguyen, Kiranbir Sodhia,
 686 Kish Greene, Lars Lowe Sjoesund, Lauren Usui, Laurent Sifre, Lena Heuermann, Leticia Lago,
 687 Lilly McNealus, Livio Baldini Soares, Logan Kilpatrick, Lucas Dixon, Luciano Martins, Machel
 688 Reid, Manvinder Singh, Mark Iverson, Martin Görner, Mat Velloso, Mateo Wirth, Matt Davidow,
 689 Matt Miller, Matthew Rahtz, Matthew Watson, Meg Risdal, Mehran Kazemi, Michael Moynihan,
 690 Ming Zhang, Minsuk Kahng, Minwoo Park, Mofi Rahman, Mohit Khatwani, Natalie Dao, Nenshad
 691 Bardoliwalla, Nesh Devanathan, Neta Dumai, Nilay Chauhan, Oscar Wahltinez, Pankil Botarda,
 692 Parker Barnes, Paul Barham, Paul Michel, Pengchong Jin, Petko Georgiev, Phil Culliton, Pradeep
 693 Kuppala, Ramona Comanescu, Ramona Merhej, Reena Jana, Reza Ardesir Rokni, Rishabh
 694 Agarwal, Ryan Mullins, Samaneh Saadat, Sara Mc Carthy, Sarah Cogan, Sarah Perrin, Sébastien
 695 M. R. Arnold, Sebastian Krause, Shengyang Dai, Shruti Garg, Shruti Sheth, Sue Ronstrom, Susan
 696 Chan, Timothy Jordan, Ting Yu, Tom Eccles, Tom Hennigan, Tomas Kociský, Tulsee Doshi,
 697 Vihan Jain, Vikas Yadav, Vilobh Meshram, Vishal Dharmadhikari, Warren Barkley, Wei Wei,
 698 Wenming Ye, Woohyun Han, Woosuk Kwon, Xiang Xu, Zhe Shen, Zhitao Gong, Zichuan Wei,
 699 Victor Cotruta, Phoebe Kirk, Anand Rao, Minh Giang, Ludovic Peran, Tris Warkentin, Eli Collins,
 700 Joelle Barral, Zoubin Ghahramani, Raia Hadsell, D. Sculley, Jeanine Banks, Anca Dragan, Slav
 701 Petrov, Oriol Vinyals, Jeff Dean, Demis Hassabis, Koray Kavukcuoglu, Clement Farabet, Elena
 Buchatskaya, Sebastian Borgeaud, Noah Fiedel, Armand Joulin, Kathleen Kenealy, Robert Dadashi,
 and Alek Andreev. Gemma 2: Improving open language models at a practical size, 2024. URL
<https://arxiv.org/abs/2408.00118>.

702 Hugo Touvron, Thibaut Lavril, Gautier Izacard, Xavier Martinet, Marie-Anne Lachaux, Timothée
 703 Lacroix, Baptiste Rozière, Naman Goyal, Eric Hambro, Faisal Azhar, et al. Llama: Open and
 704 efficient foundation language models. *arXiv preprint arXiv:2302.13971*, 2023.

705 Yanling Wang, Haoyang Li, Hao Zou, Jing Zhang, Xinlei He, Qi Li, and Ke Xu. Hidden question
 706 representations tell non-factuality within and across large language models. *arXiv e-prints*, pp.
 707 arXiv–2406, 2024.

709 Wannan Yang, Chen Sun, and Gyorgy Buzsaki. INTERPRETABILITY OF LLM DECEPTION:
 710 UNIVERSAL MOTIF. In *Neurips Safe Generative AI Workshop 2024*, 2024. URL <https://openreview.net/forum?id=DRWCDFsb2e>.

712 Lexin Zhou, Fernando Martínez-Plumed, José Hernández-Orallo, Cèsar Ferri, and Wout Schellaert.
 713 Reject before you run: Small assessors anticipate big language models. In *EBeM@IJCAI*, 2022.

715 Lexin Zhou, Pablo A. Moreno-Casares, Fernando Martínez-Plumed, John Burden, Ryan Burnell,
 716 Lucy Cheke, Cèsar Ferri, Alexandru Marcoci, Behzad Mehrbakhsh, Yael Moros-Daval, Seán Ó
 717 hÉigearthaigh, Danaja Rutar, Wout Schellaert, Konstantinos Voudouris, and José Hernández-Orallo.
 718 Predictable artificial intelligence, 2024. URL <https://arxiv.org/abs/2310.06167>.

719

720

721

722

723

724

725

726

727

728

729

730

731

732

733

734

735

736

737

738

739

740

741

742

743

744

745

746

747

748

749

750

751

752

753

754

755

756 A FURTHER RELATED WORK
757758 A.1 UNCERTAINTY QUANTIFICATION AND CONFIDENCE ESTIMATION IN LLMs
759

760 Traditional uncertainty quantification approaches for deep learning models include looking at the
761 logits of a multi-class classification network (Guo et al., 2017) or training the model to embed a
762 form of uncertainty (such as Bayesian Neural Networks, (Jospin et al., 2022) or Dropout (Gal &
763 Ghahramani, 2016)). Some of these methods can be adapted to LLMs (Shorinwa et al., 2024), for
764 instance by considering token-level output logits (Kadavath et al., 2022; Fadeeva et al., 2024) or
765 training additional modules to predict uncertainty (Kadavath et al., 2022). In simple classification tasks
766 with single-token or multiple-choice answers, these probabilities often track the LLM’s confidence.
767 However, extending these methods to open-ended answers is non-trivial, as low-level probabilities
768 do not necessarily yield a clear answer-level confidence. To this end, methods based on “semantic
769 similarity” (Kuhn et al., 2023) were proposed, but these are costly as they require the generation of
770 multiple answers from the model. A more recent approach (Sam et al., 2025) asks a set of “elicitation
771 questions” after an answer is generated and uses the responses to predict its correctness; as for
772 semantic similarity approaches, this requires repeated model queries.

773 Alternatively, LLMs can be asked to explicitly verbalize their uncertainty, with or (rarely) without
774 reference to a specific answer. For instance, (Lin et al., 2022) and Kapoor et al. (2024) finetuned
775 LLMs to numerically report their belief in the correctness of an answer, while Kadavath et al. (2022)
776 showed that older Anthropic models can verbally quantify their uncertainty about answers to multiple-
777 choice questions and finetuned the models to predict the confidence of succeeding on a question
778 without reference to a specific answer, which performed satisfactorily but struggled with novel tasks.
779 Instead, Chaudhry et al. (2024) finetuned LLMs to emit linguistic expressions of uncertainty (e.g.,
780 “maybe”). Finally, arguing that absolute verbalised confidence estimation is poor, Shrivastava et al.
781 (2025) prompted LLMs to estimate whether they are more confident in their answers to one question
782 relative to another one, then aggregate many of these pairwise comparisons into confidence scores
783 using a ranking procedure, finding small gains in discriminative power.

784 Notably, there is no consensus on the performance of these methods (Kapoor et al., 2024), which
785 were shown to be brittle to shortcuts (Heindrich et al., 2025) and to yield inconsistent results across
786 different methods (Pawitan & Holmes, 2024). In contrast to the methods above, we directly leverage
787 previously trained LLM internals *before an answer is generated*, making our method applicable to
788 free-form answers and avoiding generation from the model. Further, while sampling-based confidence
789 estimators would typically need 10-20 candidate answers per query; our probe caches activations in
790 a single forward pass, then applies a cheap linear projection. Probe training is a one-shot learning
791 of a d -dimensional parameter vector on 10 k cached activations (<3 min on CPU); applying the
792 probe involves a linear project, which is drastically lighter-weight in deployment. While the method
793 assumes white-box access, it complements black-box sampling: practitioners can choose probes
794 when speed or token budget is paramount and revert to sampling when internals are unavailable.

795 A.2 ANTICIPATING LLM PERFORMANCE

796 Our approach aims to anticipate LLM’s performance based on its internals before an answer is
797 generated. Some works (Hernández-Orallo et al., 2022; Zhou et al., 2022; Schellaert et al., 2024;
798 Pacchiardi et al., 2024; 2025) attempted to predict LLM performance by training independent
799 score predictors (“assessors”) based on features of the input question obtained independently of the
800 considered LLM. This is motivated by the idea of “Predictable AI” (Zhou et al., 2024), which argues
801 that predicting the inputs on which an AI system will behave as expected is a necessary component
802 of safety. Our work can be seen as belonging to this research strand, with the key distinction of
803 leveraging model internals, which provide more information than model-independent features.

804 A few works leveraged internals to predict models’ ability to answer a question correctly, but no work
805 has investigated directly training linear probes only relying on internals. First, Kamath et al. (2020)
806 combined embeddings generated by a model prompted with a question with hand-crafted feature and
807 the (anticipative) confidence scores of the model, and trained non-linear models (such as XGBoost)
808 to predict correctness in advance of generating answers. In contrast, our approach uses only linear
809 probes on model internals to determine whether activations from correctly and incorrectly answered
810 questions are linearly separable. More recently, Ferrando et al. (2025) contains two experiments using

810 the latent representations of SAEs (pre-trained to reconstruct model representations in unsupervised
 811 manner) on base Gemma2 2B and 9B and LLaMA 3.1 8B: in the first, they identified general
 812 “knowledge-awareness” directions that predominantly activate on known entities but not on unknown
 813 ones (and vice versa) and showed that steering the chat-fine-tuned version of the model using these
 814 directions induces hallucination or refusal. This parallels our finding that the activations lie at an
 815 extreme of the direction we identify when the model utters “I don’t know” (Section 4.5). In the
 816 second experiment, closer to our setup, they posed questions to the chat model, excluded cases where
 817 the model refuses to respond, and identified the SAE latent that has the highest difference in values
 818 between when the model produces correct and incorrect answers (“uncertainty direction”), and found
 819 good predictive power. Notably, this analysis was confined to Gemma2 models; by contrast, we
 820 directly train simple linear directions across a broader range of models, scaling up to 70 billion
 821 parameters. Nevertheless, Ferrando et al.’s approach and ours produce consistent evidence, thereby
 822 reaffirming one another.

823 Several contemporaneous works also use LLM internals to anticipate hallucination or non-factuality
 824 at question time (Snyder et al., 2024; Gottesman & Geva, 2024; Wang et al., 2024; Ji et al., 2024;
 825 Slobodkin et al., 2023). Snyder et al. (2024) and Ji et al. (2024) focus on hallucination risk and
 826 often use richer information about the generation process, such as the first generated token or short
 827 trajectories. Slobodkin et al. (2023) study (un)answerability in reading comprehension with an
 828 explicit context passage. Gottesman & Geva (2024) shift the focus to the level of entities, and
 829 estimate whether a model “knows” facts about specific entities such as historical figures. Wang
 830 et al. (2024) are closest in spirit to our work, and train more expressive classifiers over internal
 831 states to predict non-factuality and to transfer signals across models. In contrast, we deliberately
 832 adopt a stricter and simpler setting. We work with a single one-dimensional difference-of-means
 833 direction in the residual stream of one layer, trained on question-only activations before any token is
 834 generated, and we study per-question self-correctness for free-form factual QA across six open-source
 835 models from three families. This minimal probe already predicts correctness across datasets and
 836 models, which strengthens the claim that a linearly accessible correctness or confidence signal exists
 837 in mid-late layers.

839 A.3 PROBING OTHER PROPERTIES WITH MODEL INTERNALS

840
 841 Closely related to our work is the growing literature on using hidden activations to detect properties
 842 of the model’s upcoming or generated outputs. Several papers (Burns et al., 2022; Azaria & Mitchell,
 843 2023; Marks & Tegmark, 2023; Burger et al., 2024; Bao et al., 2025) showed that linear or shallow
 844 probes on internal representations can detect whether a full statement (or question+answer) processed
 845 by the model is true or false. Analogously to our findings, Bao et al. (2025) found that more capable
 846 models have stronger representations, and that probes trained on atomic statements generalise to
 847 more complex sentences. This is closely related to Concept Activation Vectors (Kim et al., 2018) in
 848 explainable AI, which describe a model’s internal representations in terms of its sensitivity to user-
 849 defined examples for a concept. Our approach chiefly differs from those mentioned above by relying
 850 on the activations obtained *in advance* of the model generating an answer to a question. Experiments
 851 in this setup were conducted (among other things) in Kadavath et al. (2022) for proprietary models.
 852 Our work corroborates their promising results with evidence from newer open-source LLMs.

853 Other works extracted other information from internals. For instance, Heindrich et al. (2025) predicted
 854 question answerability. Our work focuses on correctness, which encapsulates when a question is
 855 possibly answerable but the model is incorrect. Kudo et al. (2024) studied internals across models’
 856 chain of thought and analyse when they start predicting the answer the model eventually produces;
 857 in contrast, we study whether the internals predict *correctness* of the answer. Goldowsky-Dill
 858 et al. (2025) studied the detection of deception (a model deliberately misleading its interlocutor);
 859 correctness is broader, and less dependent on the fragile role-play setting required to elicit such
 860 deceptive behaviour. It is worth noting that Parrack et al. (2025) found white box probes to be
 861 slightly better than black-box detection approaches. Relatedly, Yang et al. (2024) analyse how LLMs
 862 internally separate truthful vs. lying scenarios (with the model instructed to lie) at different layers,
 863 using dimensionality reduction and intervention experiments (“patching” activations from a lying
 864 scenario into a truthful one). Instead, (Nguyen et al., 2025) show that linear probes can separate tasks
 865 encountered during evaluations and deployment.

Finally, Lee et al. (2025) used activation steering to condition models to refuse harmful prompts; our work focuses on correctness rather than harmfulness, which requires understanding one's own capabilities. In certain cases, we expect correctness to be a prerequisite to harmfulness, as incorrectly answering a banal question may be harmful but correctly answering it may be completely safe. Beaglehole et al. (2025) conducted a similar steering study, detecting semantic concepts using non-linear feature learning and aggregating features across layers. In contrast, we show that correctness, a particularly important semantic concept, can be captured using linear features in individual layers, indicating that the concept is strongly present and can be easily accessed by the model.

B ADDITIONAL QUANTITATIVE RESULTS

B.1 LLM PERFORMANCE ON DATASETS

Table 5 reports performance of all models on each dataset with the prompts we used (Appendix B.8).

Table 5: Model performance across tasks (%).

Model	TriviaQA	N. people	Cities	Math ops.	Medals	GSM8K
Llama 3.1 8B	85.6	93.4	67.4	77.5	46.0	13.3
Mistral 7B Instruct v0.3	83.6	84.7	45.8	73.9	42.8	10.7
Llama 3.3 70B Instruct	93.4	97.6	80.3	82.2	83.5	36.3
Qwen 2.5 7B Instruct	73.8	42.8	62.9	80.8	29.8	36.0
Minstral 8B Instruct 2410	79.9	67.4	73.0	74.2	40.5	14.8
DeepSeek R1 Distill Qwen 32B	59.9	50.8	60.3	82.0	33.0	44.3

B.2 EXTENDED INFORMATION ON THE DIRECTION APPROACH

Extended experimental results on the direction approach are provided in this section, offering further context that was not included in the main text. Table 6 extends the results of the direction approach presented in Table 3 and Table 7 provides the accuracy on all test datasets of a potential classifier derived from the correctness direction.

Table 8 shows the AUROC values on the model optimal layer (from Section 4.2) and the AUROC values on the layer optimized per dataset for all models and datasets. This comparison demonstrates that the single model-optimal layer is already highly effective, achieving performance very close to the dataset-specific optimal layer.

Table 6: Mean and standard deviation AUROC of the 5 folds for the direction approach (Section 3.2) for each dataset and model. All directions are trained on the TriviaQA dataset on the optimal layer found in Section 4.2.

Model	Test dataset					
	TriviaQA	N. people	Cities	Math ops.	Medals	GSM8K
Llama 3.1 8B	0.804 ± 0.006	0.722 ± 0.010	0.732 ± 0.018	0.858 ± 0.027	0.680 ± 0.007	0.534 ± 0.022
Llama 3.3 70B	0.826 ± 0.006	0.708 ± 0.018	0.880 ± 0.014	0.835 ± 0.031	0.770 ± 0.022	0.499 ± 0.015
Qwen 2.5 7B	0.758 ± 0.006	0.800 ± 0.013	0.842 ± 0.008	0.837 ± 0.032	0.586 ± 0.014	0.601 ± 0.015
Deepseek R1 32B	0.735 ± 0.005	0.825 ± 0.008	0.879 ± 0.007	0.847 ± 0.035	0.638 ± 0.020	0.552 ± 0.012
Mistral 7B	0.796 ± 0.009	0.760 ± 0.016	0.880 ± 0.008	0.782 ± 0.033	0.645 ± 0.005	0.579 ± 0.016
Minstral 8B	0.734 ± 0.004	0.680 ± 0.007	0.840 ± 0.021	0.844 ± 0.020	0.670 ± 0.015	0.578 ± 0.013

B.3 ASSESSORS PERFORMANCE

For the gradient boosted decision tree assessors, we used XGBoost (Chen & Guestrin, 2016). The number of trees were chosen individually for each model by performing 5-fold cross validation on the same training subset of TriviaQA as in Section 4.3. The rest of XGBoost's hyperparameters were left as default.

918
 919 Table 7: Accuracy of a classifier based on the correctness direction at the optimal layer from Section
 920 4.2. For each test dataset, we display results for the direction trained on TriviaQA and for the direction
 921 trained on the dataset itself. The threshold for the classifier is chosen using only training data.

922 Model 923 Trained with	Test dataset											
	TriviaQA		N. people		Cities		Math ops.		Medals		GSM8K	
924 TriviaQA	925 Itself	926 TriviaQA	927 Itself	928 TriviaQA	929 Itself	930 TriviaQA	931 Itself	932 TriviaQA	933 Itself	934 TriviaQA	935 Itself	
Llama 3.1 8B	0.728	0.728	0.522	0.688	0.551	0.714	0.755	0.874	0.612	0.682	0.500	0.670
Llama 3.3 70B	0.750	0.750	0.621	0.651	0.797	0.808	0.520	0.943	0.553	0.782	0.500	0.671
Qwen 2.5 7B	0.688	0.688	0.639	0.764	0.515	0.762	0.792	0.938	0.512	0.640	0.501	0.654
Deepseek R1 32B	0.671	0.671	0.588	0.793	0.612	0.802	0.848	0.961	0.519	0.636	0.500	0.660
Mistral 7B	0.721	0.721	0.523	0.724	0.771	0.811	0.724	0.858	0.545	0.661	0.503	0.659
Minstral 8B	0.670	0.670	0.514	0.647	0.500	0.774	0.764	0.830	0.532	0.656	0.502	0.671

930
 931 Table 8: AUROC values on the model optimal layer from Section 4.2 and on the layer optimized per
 932 dataset for all models and datasets.

933 Model 934 Opt. layer over	Test dataset											
	TriviaQA		Cities		Math ops.		Medals		GSM8K			
935 Model	936 Dataset	937 Model	938 Dataset	939 Model	940 Dataset	941 Model	942 Dataset	943 Model	944 Dataset	945 Model	946 Dataset	
Llama 3.1 8B	Layer AUROC	14 0.802	16 0.803	14 0.732	30 0.783	14 0.860	12 0.901	14 0.677	28 0.712	14 0.537	12 0.548	
Llama 3.3 70B	Layer AUROC	76 0.821	76 0.821	76 0.881	72 0.890	76 0.835	32 0.979	76 0.772	40 0.794	76 0.499	32 0.625	
Qwen 2.5 7B	Layer AUROC	22 0.760	22 0.760	22 0.841	20 0.854	22 0.833	20 0.875	22 0.587	20 0.588	22 0.602	20 0.678	
Deepseek R1 32B	Layer AUROC	44 0.734	44 0.734	44 0.880	48 0.890	44 0.848	52 0.963	44 0.640	48 0.665	44 0.554	12 0.642	
Mistral 7B	Layer AUROC	16 0.798	16 0.798	16 0.879	30 0.914	16 0.801	22 0.915	16 0.647	20 0.699	16 0.579	18 0.592	
Minstral 8B	Layer AUROC	18 0.738	18 0.738	18 0.840	16 0.846	18 0.843	16 0.859	18 0.666	16 0.669	18 0.574	2 0.637	

947
 948 Table 9: AUROC for logistic regression and Gradient Boosted Decision Tree (XGBoost) assessors.

949 Model	950 Assessor	Test dataset							
		951 TriviaQA	952 N. people	953 Cities	954 Math ops.	955 Medals	956 GSM8K	957 Model	958 Dataset
Llama 3.1 8B	Log. regression XGBoost (133 trees)	0.852 0.896	0.630 0.560	0.663 0.639	0.528 0.453	0.623 0.554	0.558 0.532		
Llama 3.3 70B	Log. regression Instruct XGBoost (150 trees)	0.759 0.853	0.583 0.516	0.672 0.608	0.449 0.398	0.568 0.501	0.573 0.543		
Qwen 2.5 7B	Log. regression Instruct XGBoost (47 trees)	0.807 0.847	0.723 0.619	0.708 0.624	0.400 0.506	0.622 0.580	0.584 0.546		
DeepSeek R1	Log. regression	0.790	0.709	0.663	0.337	0.601	0.576		
Distill Qwen 32B	XGBoost (51 trees)	0.834	0.608	0.609	0.458	0.547	0.541		
Mistral 7B	Log. regression	0.846	0.673	0.710	0.493	0.638	0.559		
Instruct v0.3	XGBoost (130 trees)	0.898	0.558	0.672	0.380	0.590	0.543		
Minstral 8B	Log. regression	0.789	0.623	0.682	0.454	0.626	0.598		
Instruct 2410	XGBoost (65 trees)	0.846	0.545	0.611	0.498	0.551	0.556		

964 965 966 B.4 HOW MUCH TRAINING DATA DO WE NEED TO LEARN THE CORRECTNESS DIRECTION?

967
 968 Figure 5 shows performance for the correctness direction trained on TriviaQA for an increasing
 969 number of training samples. Interestingly, Mathematical Operations has the highest data complexity,
 970 likely due to the fact that arithmetic errors are heterogeneous and need a large amount of averaging out
 971 to cancel the variance of the activations.

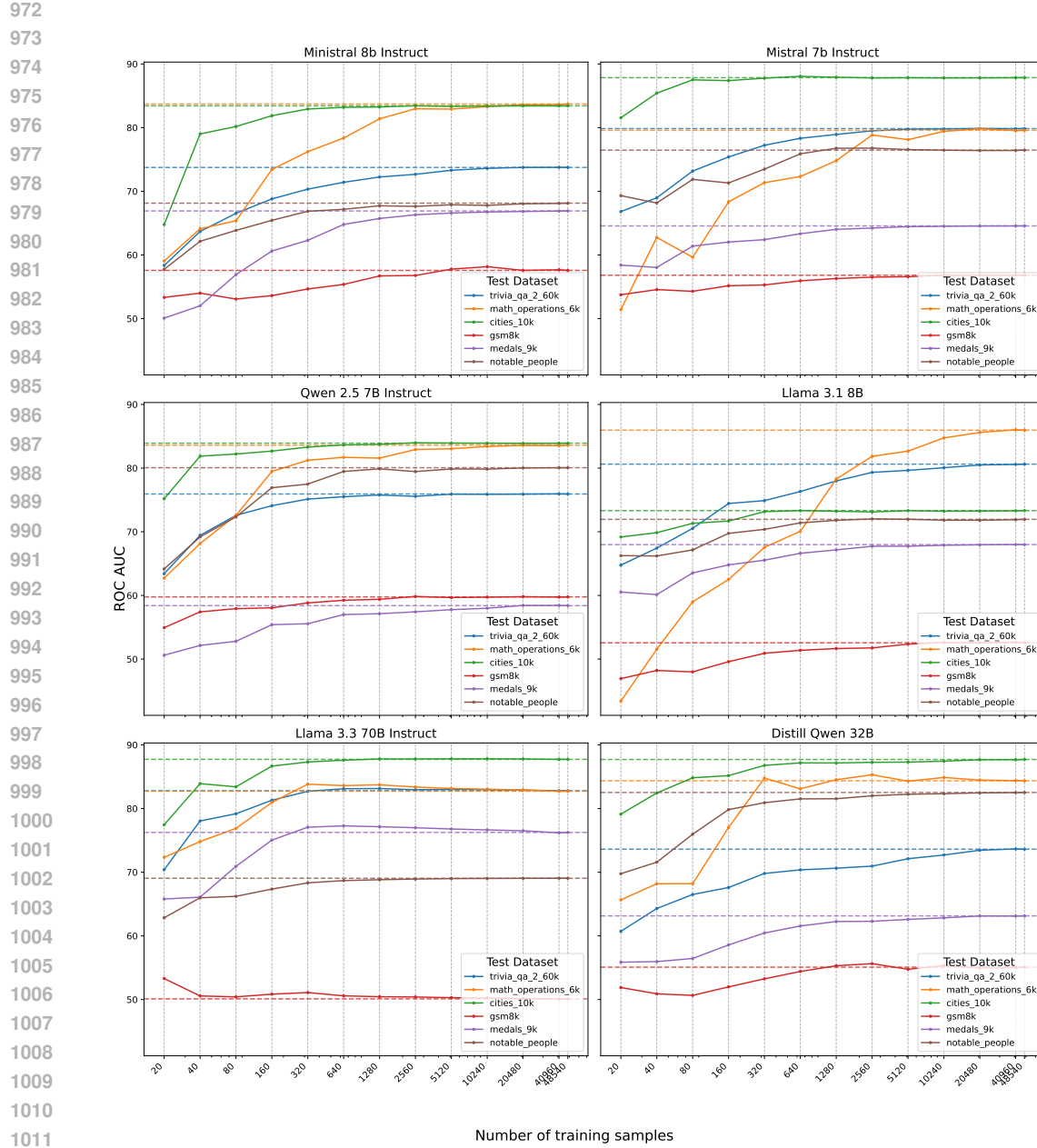


Figure 5: AUROC scores for each model and test dataset for different number of training samples from TriviaQA, for our correctness direction approach. To reduce variance, 10 experiments were performed for each number of training samples and the average AUROC is reported. Notice that the x scale is logarithmic.

B.5 HEATMAPS

Figure 6 and Figure 7 complement Figure 3 from the main text and reports AUROC mean and standard deviation scores for each combination of model, train dataset and test dataset.

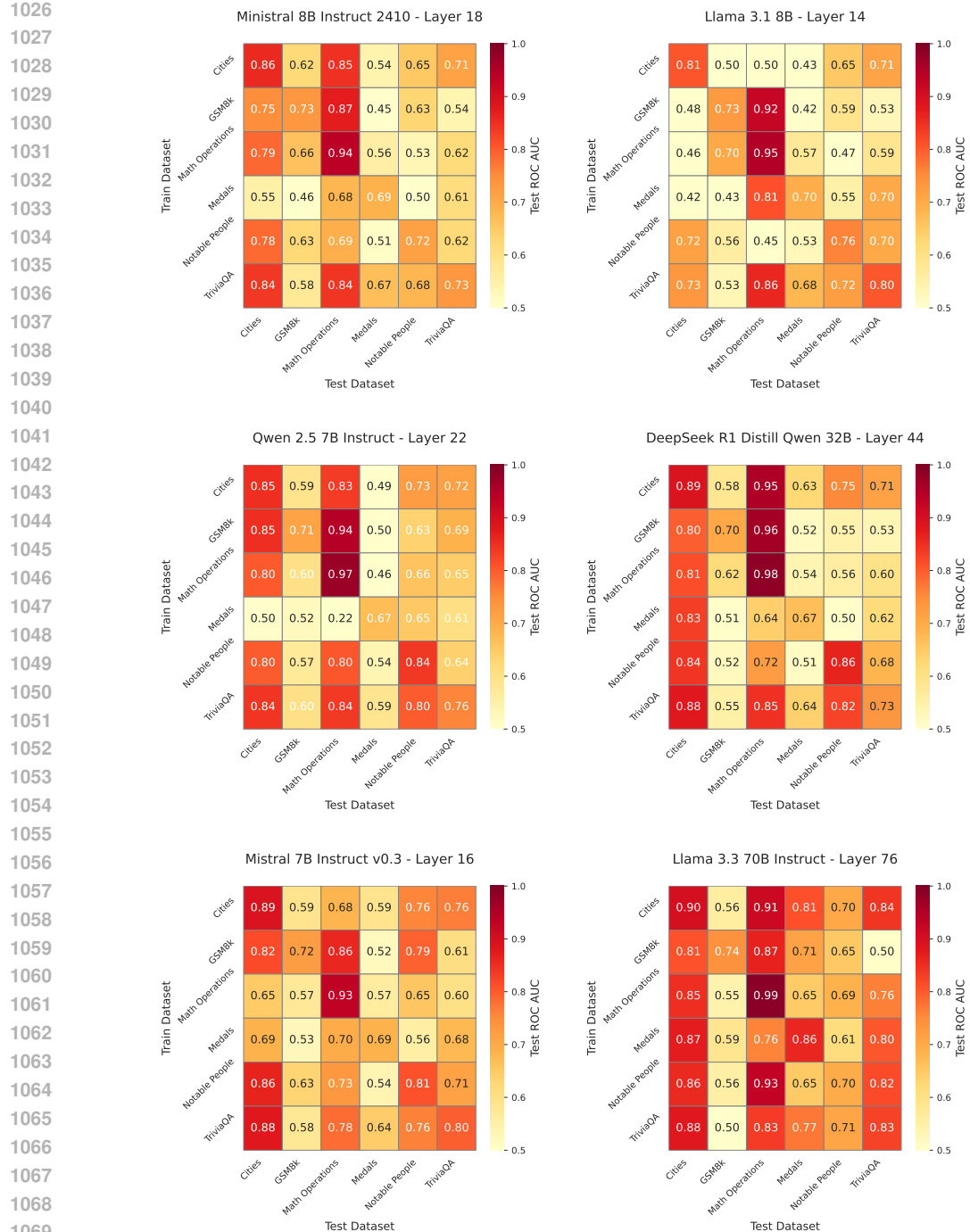
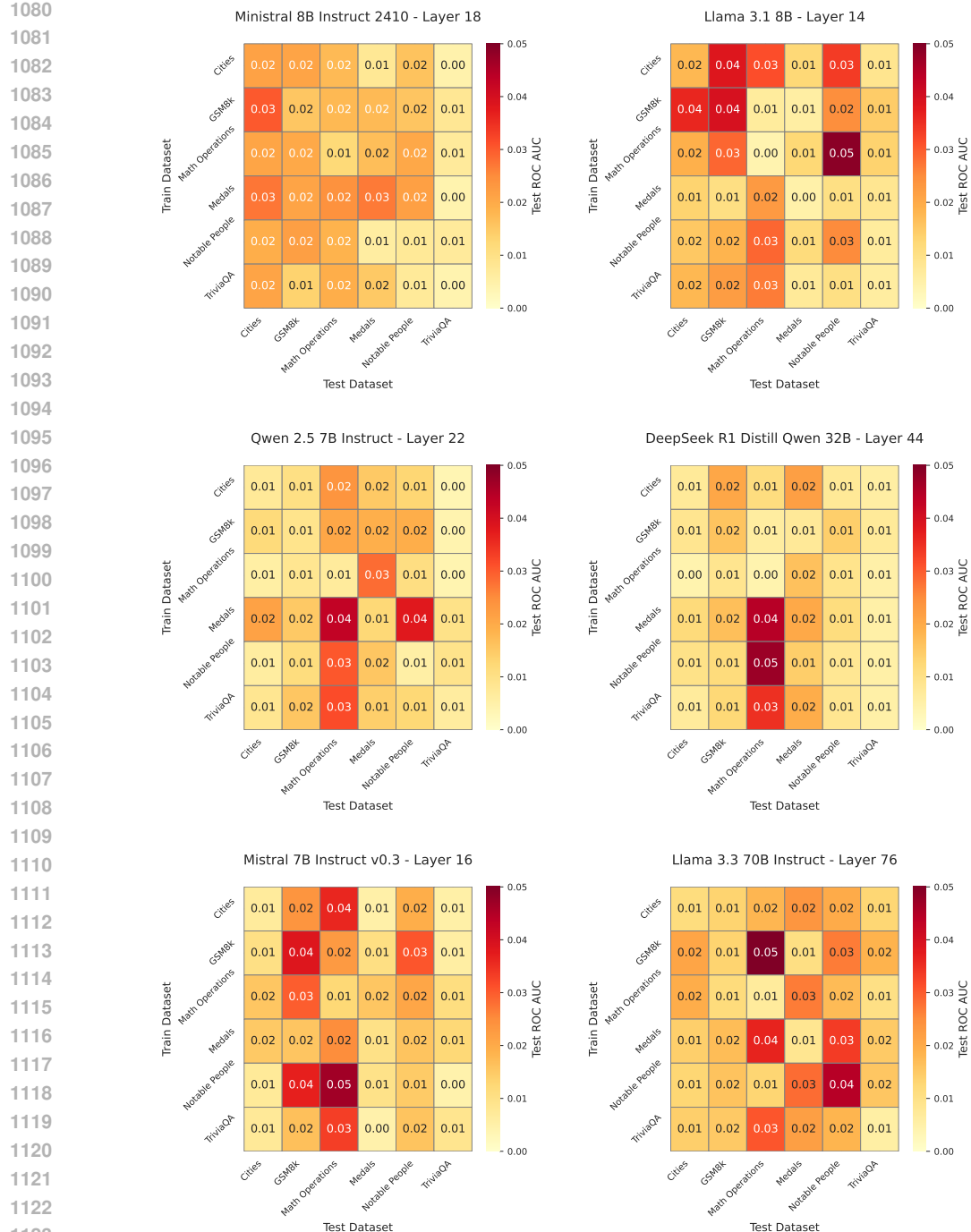


Figure 6: AUROC scores on each dataset for the direction learned on each dataset individually for all models. Average AUROC over 5 folds is reported (Section 4.3).



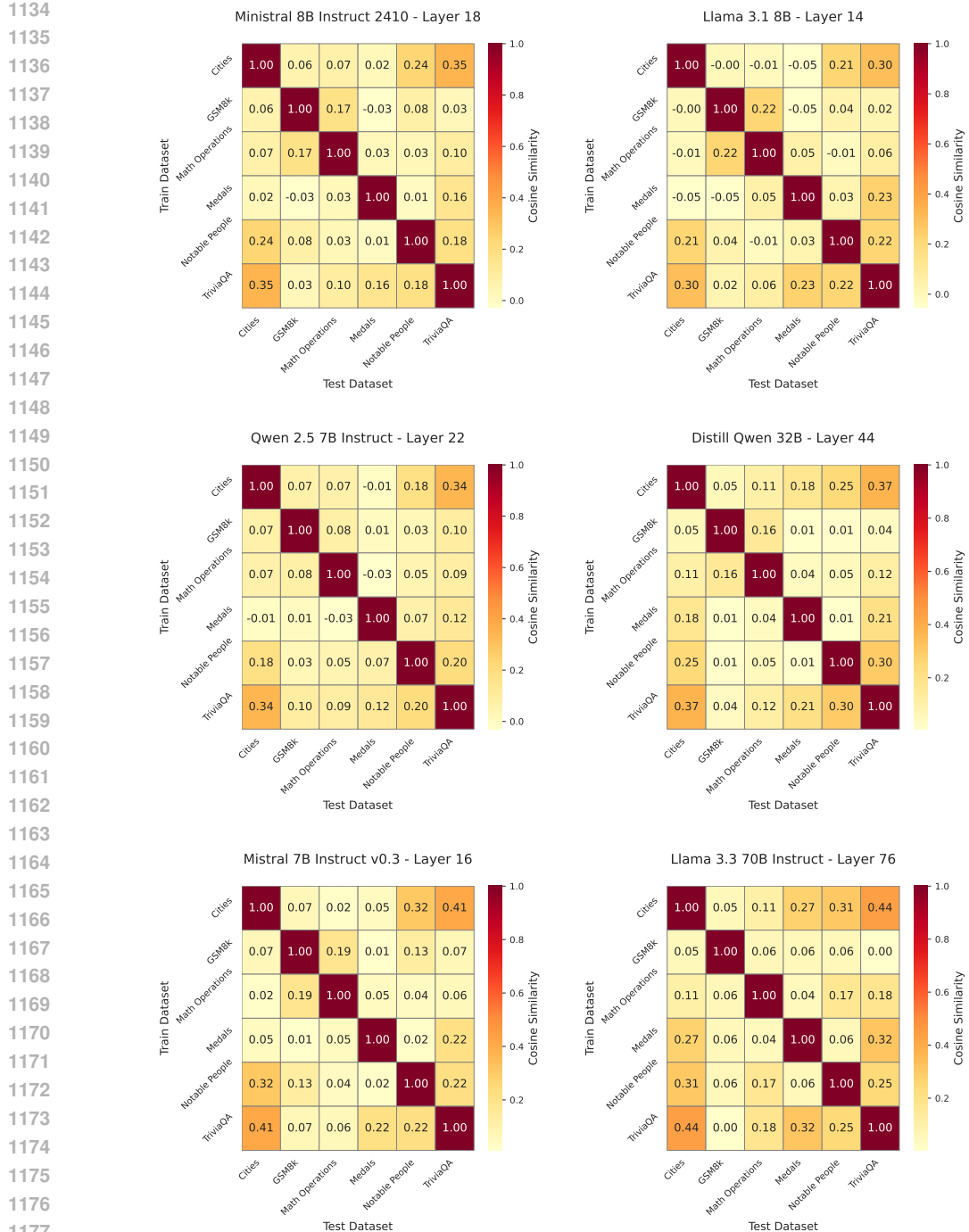


Figure 8: Cosine similarities for directions trained with different datasets. Following the same method as in Section 4.3, we average the directions over 5 folds and provide cosine similarities for these averages.

B.7 CORRECTNESS DIRECTION PERFORMANCE ACROSS LAYERS

Figure 9 shows the in-distribution performance of the direction trained on each dataset over the layers of each considered model, complementing Figure 2.

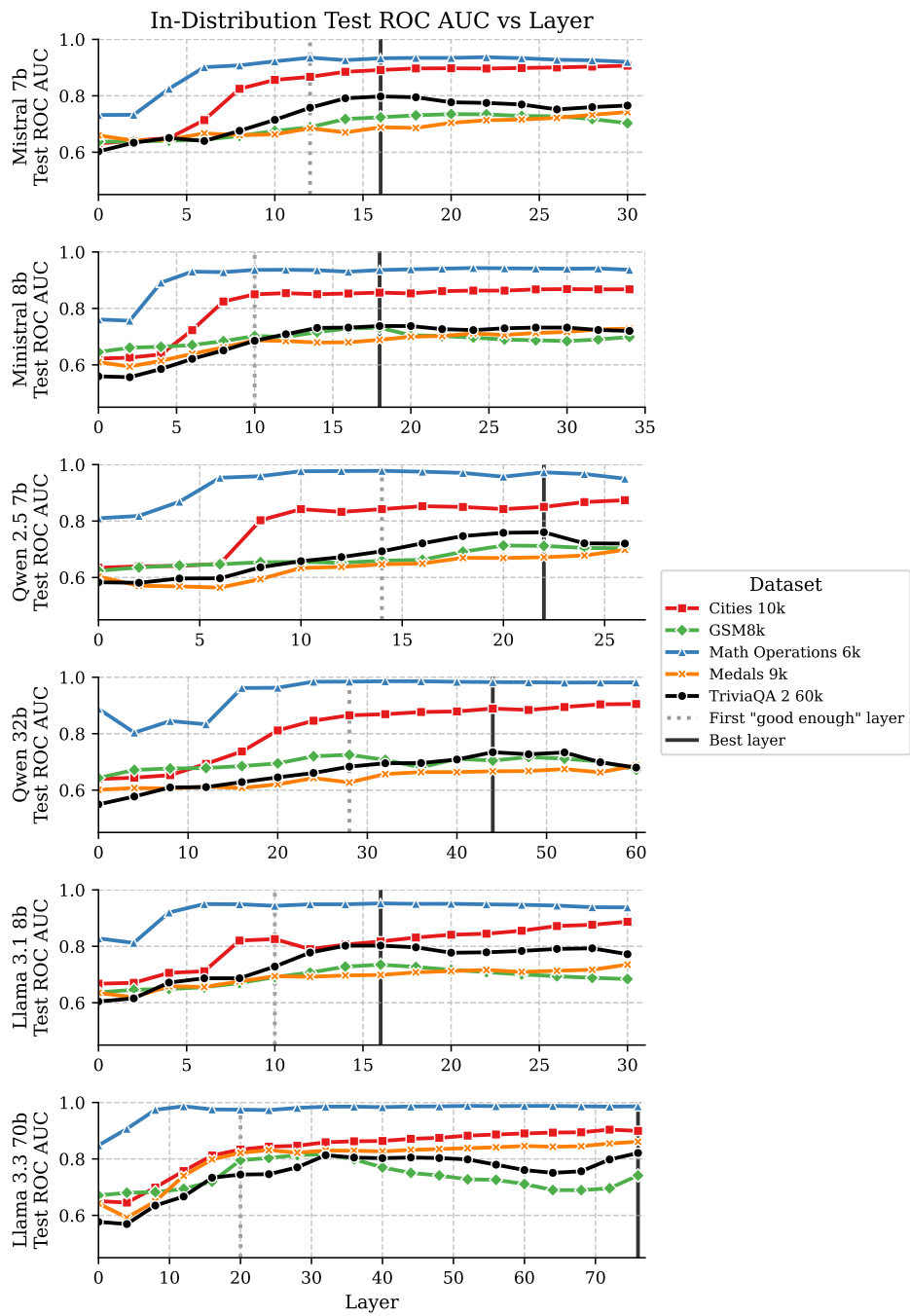


Figure 9: AUROC for each dataset, model and layer for the direction approach explained in Sec 3.2. The direction is trained and tested on the same dataset (using cross-validation). We collect activations every 2 layers for small ($<10B$ parameters) models and every 4 layers for large ($>10B$ parameters) models. The best layer is chosen as in Section 4.2, and the first "good enough" layer is the first layer that achieves 90% of the accuracy of the best layer in TriviaQA.

1242 B.8 PROMPTS

1243

1244 Below we report the prompts used for our evaluations.

1245

1246 Prompt for Cities dataset:

1247

1248 I am going to ask you a question about cities. End your sentence with {eos_token}.Here are
1249 some examples of questions that might help you:

1250

Question: In which country is the city of Barcelona located?

Answer: Spain{eos_token}

1252

Question: In which country is the city of London located?

Answer: United Kingdom{eos_token}

1255

Question: In which country is the city of Beijing located?

Answer: China{eos_token}

1256

Question:{question}

Answer:

1261

Prompt for Notable People dataset:

1262

I am going to ask you what year a person was born. End your sentence with {eos_token}.Here
1264 are some examples of questions that might help you:

1265

Question: What year was Barack Obama (politician from US) born?

Answer: 1961{eos_token}

1266

Question: What year was Vladimir Putin (politician from Russia) born?

Answer: 1952{eos_token}

1267

Question: What year was Xi Jinping (politician from China) born?

Answer: 1953{eos_token}

1268

Question:{question}

Answer:

1269

Prompt for Medals dataset:

1270

I am going to ask you a question about the Olympics. End your sentence with
1279 {eos_token}.Here are some examples of questions that might help you:

1280

Question: Which country won gold in Gymnastics Women's Team All-Around in the 1928 Summer
1282 Olympics?

Answer: Netherlands{eos_token}

1283

Question: Which country won gold in Hockey Women's Hockey in the 2004 Summer Olympics?

Answer: Germany{eos_token}

1284

Question: Which country won gold in Fencing Men's Sabre, Individual in the 1964 Summer
1286 Olympics?

Answer: Hungary{eos_token}

1287

Question:{question}

Answer:

1288

Prompt for TriviaQA dataset:

1295

1296 I am going to ask you a question. Answer concisely. End your sentence with {eos_token}.Here
 1297 are some examples of questions that might help you:
 1298

1299 Question: In which month are St David's Day and St Patrick's Day celebrated in the UK?
 1300 Answer: March{eos_token}

1302 Question: What is the common English name of Mozart's Serenade for Strings in d major?
 1303 Answer: A little night music{eos_token}

1304 Question: In which US State do teams play baseball in the Cactus League?
 1305 Answer: Arizona{eos_token}

1307 Question:{question}
 1308 Answer:

1310 Prompt for Math Operations dataset:
 1311

1312 I am going to ask you questions about maths. Answer with an integer value, without decimal
 1313 places. End your sentence with {eos_token}.Here are some examples of questions that might
 1314 help you:
 1315

1316 Question: What is 604 minus 866?
 1317 Answer: -262{eos_token}

1319 Question: What is 927 plus 855?
 1320 Answer: 1782{eos_token}

1322 Question: What is 531 times 955?
 1323 Answer: 507105{eos_token}

1325 Question:{question}
 1326 Answer:

1327 Prompt for GSM8K dataset:
 1328

1329 I am going to ask you a question that requires your answer in a boxed integer. End your sentence
 1330 with {eos_token}.Here are some examples of questions that might help you:
 1331

1332 Question: Weng earns \$12 an hour for babysitting. Yesterday, she just did 50 minutes of babysitting.
 1333 How much did she earn?
 1334 Answer: \$\boxed{10}\${eos_token}

1336 Question: Julie is reading a 120-page book. Yesterday, she was able to read 12 pages and today,
 1337 she read twice as many pages as yesterday. If she wants to read half of the remaining pages
 1338 tomorrow, how many pages should she read?
 1339 Answer: \$\boxed{42}\${eos_token}

1341 Question: Mark has a garden with flowers. He planted plants of three different colors in it. Ten of
 1342 them are yellow, and there are 80% more of those in purple. There are only 25% as many green
 1343 flowers as there are yellow and purple flowers. How many flowers does Mark have in his garden?
 1344 Answer: \$\boxed{35}\${eos_token}

1345 Question:{question}
 1346 Answer:

1348 Prompt for the verbalized confidence experiment:
 1349

1350
1351 I am going to ask you about your confidence to answer a question. The confidence indicates how
1352 likely you think your answer will be true. Please respond with only a percentage and end with
1353 {eos_token}, so your answer should be following the format
1354

Answer: (percentage)%{eos_token}

1355 How confident are you that you can answer correctly '{question}'? Answer:
1356

1357 C THE USE OF LARGE LANGUAGE MODELS IN THIS RESEARCH PAPER 1358

1359 Besides being the subject of the investigation, the authors acknowledge having used Large Language
1360 Models in polishing the writing of some sections and for finding related works to be mentioned.
1361

1362

1363

1364

1365

1366

1367

1368

1369

1370

1371

1372

1373

1374

1375

1376

1377

1378

1379

1380

1381

1382

1383

1384

1385

1386

1387

1388

1389

1390

1391

1392

1393

1394

1395

1396

1397

1398

1399

1400

1401

1402

1403